

Inactivation of the Quinone Oxidoreductases NQO1 and NQO2 Strongly Elevates the Incidence and Multiplicity of Chemically Induced Skin Tumors

Jun Shen¹, Roberto J. Barrios², and Anil K. Jaiswal¹

Abstract

The cytosolic quinone oxidoreductases NQO1 and NQO2 protect cells against oxidative stress by detoxifying quinones and preventing redox cycling. In this study, we used double knockout (DKO) mice deficient for NQO1 and NQO2 to investigate the role of these antioxidative enzymes in a two-stage model of inflammatory skin carcinogenesis. In this model, tumors are caused by exposure to topical carcinogen dimethylbenz(a)anthracene or benzo(a)pyrene (BP) followed by twice weekly application of proinflammatory phorbol 12-myristate 13-acetate. On this classic chemical carcinogenesis protocol, DKO mice showed a significantly higher skin tumor frequency and multiplicity compared with control wild-type or single knockout mice. Analysis of skin from wild-type and DKO mice exposed to BP for 6, 12, or 24 hours revealed a relative delay in the activation of p53, p63, p19ARF, and apoptosis in DKO mice, consistent with a negative modifier role for NQO1/NQO2 in carcinogenesis. Our findings offer genetic evidence of the significance of quinone oxidoreductases NQO1 and NQO2 in limiting chemical skin carcinogenesis. *Cancer Res*; 70(3); 1006–14. ©2010 AACR.

Introduction

Polycyclic aromatic hydrocarbons (PAH) such as 7,12-dimethylbenz(a)anthracene (DMBA) and benzo(a)pyrene (BP) are known environmental contaminants. They are present in tobacco smoke and motor vehicle exhaust and produced during burning of carbohydrates, fat, and protein (1, 2). DMBA and BP both are recognized mutagens and carcinogens in human and rodents (2, 3). The incidence of skin cancer is equivalent to the incidence of malignancies in all other organs combined and thus represents a major, and growing, public health problem (4).

Dicoumarol-sensitive NAD(P)H:quinone oxidoreductase (NQO1) is a flavoprotein that catalyzes metabolic detoxification of quinones, leading to protection against oxidative stress (5). However, NQO1 in many instances has been reported to activate drugs, leading to cell death (5). NRH:quinone oxidoreductase 2 (NQO2) is a second member of the quinone oxidoreductases (5). The cofactor requirement for activity is very selective, requiring NAD(P)H for NQO1 and dihydronicotinamide riboside (NRH) for NQO2 (6, 7). NQO2 is inhibited by flavones such as quercetin (6) and BP (7). Although overlapping substrate specificities have been observed for NQO1 and NQO2, such as for CB1954 activation,

significant differences exist in relative affinities for the various substrates (6–8).

NQO1^{-/-} and NQO2^{-/-} mice were generated (9, 10). The mice were born normal but showed altered intracellular redox status; altered metabolism of carbohydrates, fatty acids, and nucleotides; and reduced accumulation of abdominal fat with age (11). The studies also showed that disruption of the *NQO1* gene in mice led to myelogenous hyperplasia of bone marrow and increased sensitivity of NQO1^{-/-} mice to menadione-induced hepatic damage (12). Similar to NQO1^{-/-} mice, myeloid hyperplasia of bone marrow was detected in NQO2^{-/-} mice (10). NQO1^{-/-} and NQO2^{-/-} mice also showed increased sensitivity to skin carcinogenesis in response to BP and DMBA (13–16).

The human NQO1 and NQO2 genes are precisely located on chromosomes 16q22 and 6p25, respectively (17). The C-T polymorphism in the human NQO1 gene produces a proline to serine (P187S) substitution that inactivates the enzyme (18). NQO1P187S is associated with greater risk of neutropenia in benzene-exposed adult Chinese workers (19) and is significantly overexpressed in therapy-related and *de novo* leukemias in adults (20). The human NQO2 gene locus is highly polymorphic (17, 21, 22). Among these, a 29-bp insertion/deletion promoter polymorphism associated with altered expression of the NQO2 gene and Parkinson disease is especially notable (23, 24). The studies have shown that a substantial number of human individuals carrying mutations in both NQO1 and NQO2 genes have reduced levels of these enzymes (25). The susceptibility of these individuals to diseases remains unknown (25).

The development of skin cancer is a multistage process that includes initiation, promotion, and progression in experimental animal models and induction and propagation possibly in human cancer (26). To examine the combined *in vivo*

Authors' Affiliations: ¹Department of Pharmacology and Experimental Therapeutics, University of Maryland School of Medicine, Baltimore, Maryland and ²Department of Pathology, Methodist Hospital, Houston, Texas

Corresponding Author: Anil K. Jaiswal, Department of Pharmacology and Experimental Therapeutics, University of Maryland School of Medicine, 655 West Baltimore Street, Baltimore, MD 21201. Phone: 410-706-2285; Fax: 410-706-5692; E-mail: ajaiswal@som.umaryland.edu.

doi: 10.1158/0008-5472.CAN-09-2938

©2010 American Association for Cancer Research.

role of NQO1 and NQO2, double knockout (DKO) NQO1^{-/-} NQO2^{-/-} mice were generated by cross-breeding NQO1^{-/-} mice with NQO2^{-/-} mice (25). DKO mice showed significantly higher sensitivity to DMBA- and BP-induced skin carcinogenesis, especially tumor multiplicity, as compared with wild-type (WT) and individual knockout mice. The results also suggest that delayed activation of p63/p53/p19 and decreased apoptosis contributed to increase in skin tumors in DKO mice. The results together suggest that NQO1 and NQO2 combined protect against DMBA- and BP-induced skin carcinogenesis.

Materials and Methods

WT and DKO mice. C57BL/6 NQO1^{-/-}, NQO2^{-/-}, and DKO NQO1^{-/-}/NQO2^{-/-} mice were generated in our laboratory. The WT and DKO mice were housed in polycarbonate cages in the animal facility at the University of Maryland (Baltimore, MD). The mice were kept in an air-conditioned barrier facility at a temperature of 24 ± 2°C and a humidity of 55 ± 5% with a 12:12 light-dark cycle. Mice were fed standard rodent chow and acidified tap water *ad libitum*. Six- to 8-wk-old mice were used for the experiments in this study. The University of Maryland Baltimore Institutional Animal Care and Use Committee approved the study and safety protocol. The animals received humane care throughout the experiment.

DMBA- and BP-induced skin carcinogenesis. Six- to 8-wk-old C57BL/6 WT and DKO mice deficient in NQO1 and NQO2 were used. The lower backs of mice were shaved using hair clippers. Twenty to 24 mice (half male and half female) were used in each group. The various concentrations of DMBA (200, 400, and 600 nmol) or 800 nmol of BP in acetone were applied on mice skin 2 d after shaving. The control mice received acetone alone. This was followed by twice-weekly applications of 10 µg phorbol 12-myristate 13-acetate (PMA) for 20 wk starting at 1 wk after DMBA treatment. Five NQO1^{-/-} and five NQO2^{-/-} mice were included in each group for comparison with DKO mice. Mice were observed weekly for development of skin tumors. Skin tumor formation was recorded weekly, and tumors >1 mm in diameter were included in the cumulative total if they persisted for >2 wk.

Histologic examination of DMBA- and BP-induced skin tumors. Mice were sacrificed if moribund, or any individual tumor reached a diameter of 4 mm, or at the termination of the experiment (30th week). The skin tumor specimens were collected and fixed in 10% buffered formalin overnight and embedded in paraffin, sectioned at ~4 µm, and stained with H&E. Diagnostic criteria for skin tumors were based on expert pathologist reports and the available literature (26). *Pathology of tumours in laboratory animals, volume 2—tumours of the mouse* (27) was also consulted. Histopathologic lesions of the skin epidermal tumors were classified into squamous cell papilloma, keratoacanthoma, squamous cell carcinoma, and basal cell tumor.

Immunohistochemistry and Western blot analysis of skin exposed to BP. Six- to 8-wk-old C57BL/6 WT and

DKO mice were used. The lower backs of the skin were shaved using hair clippers. Two days later, acetone and 800 nmol of BP dissolved in 100 µL acetone were applied on the shaved mice skin. The control mice received acetone only. Six, 12, 24, and 48 h later, WT and DKO mice were euthanized. Skin samples were removed by surgery.

A portion of skin tissue was used for immunohistochemical analysis. The skin tissues were fixed in 10% buffered formalin overnight and embedded in paraffin and sectioned at ~4 µm. The skin slides for short-term study were deparaffinized in xylenes and rehydrated in graded alcohol and PBS followed by immunohistochemical analysis with Immunoperoxidase Secondary Detection System (Chemicon). Briefly, endogenous peroxidase was quenched by treatment of skin sections with 3% hydrogen peroxide for 10 min. The slides were heated in a boiled 0.01 mol/L citrated buffer (pH 6.0; BD Biosciences) by a microwave oven for 3 min to unmask antigen. Tissue sections were blocked with blocking reagent containing 5% normal goat serum for 30 min. After blocking, rabbit anti-mouse p53 (diluted 1:500; CM5p; Novocastra Laboratories), p63 (4A4; 1:1,000), Bax (P-19; 1:50), Bcl2 (N-19; 1:50; Santa Cruz Biotechnology), caspase-3 (1:250; Cell Signaling Technology, Inc.), and ornithine decarboxylase (ODC; 1:50; Sigma Chemical Co.) were added and incubated overnight at 4°C in a humid chamber. The slides were washed and incubated with goat anti-rabbit or goat anti-mouse secondary antibody (30 min). This was followed by washing of slides and incubation with horseradish peroxidase (HRP) reagents (15 min). Then, the slides were exposed to 3,3'-diaminobenzidine substrate and counterstained with Mayer's hematoxylin. For nuclear staining of p53 and p63, positive cells were examined, photographed, and counted from 15 different fields from three mice.

The remaining skin tissues were homogenized in an ice-cold buffer containing 150 mmol/L NaCl, 1% NP40, 0.5% deoxycholate, 0.1% SDS, and 0.5% Triton X-100 in 50 mmol/L Tris (pH 7.4) and a mixture of protease inhibitors including 1 mmol/L phenylmethylsulfonyl fluoride, 1 mmol/L DTT, 1 µg/mL pepstatin, aprotinin, leupeptin, and antipain (all from Sigma Chemical). Skin protein samples (50–100 µg) were separated on 10% to 12% SDS-PAGE and transferred to nitrocellulose membranes and probed with antibodies against NQO1 (diluted 1:1,000; generated from our laboratory); NQO2 (N-15; 1:250), p53 (DO-1; 1:1,000), c-Jun (H-79; 1:250), Bcl2 (N-19; 1:500), Bax (P-19; 1:500), and p19 (E-11; 1:250; Santa Cruz Biotechnology); p21 (1:1,000) and proliferating cell nuclear antigen (PCNA; 1:1,000; BD Biosciences); caspase-3 (1:500; Cell Signaling Technology); anti-poly (ADP-ribose) polymerase (PARP) p85 fragment polyclonal antibody (1:250; Promega); and ODC (1:250) and β-actin (1:5,000; Sigma Chemical). Immunoblots were incubated with a HRP-conjugated secondary antibody (goat anti-mouse IgG HRP, goat anti-rabbit IgG HRP, and rabbit anti-goat IgG HRP, diluted 1:2,000; Chemicon) with enhanced chemiluminescence (GE Healthcare) reagents by the procedures suggested by the manufacturer.

Statistical analysis. Data for tumor incidence, multiplicities, and average positive cell numbers were analyzed by

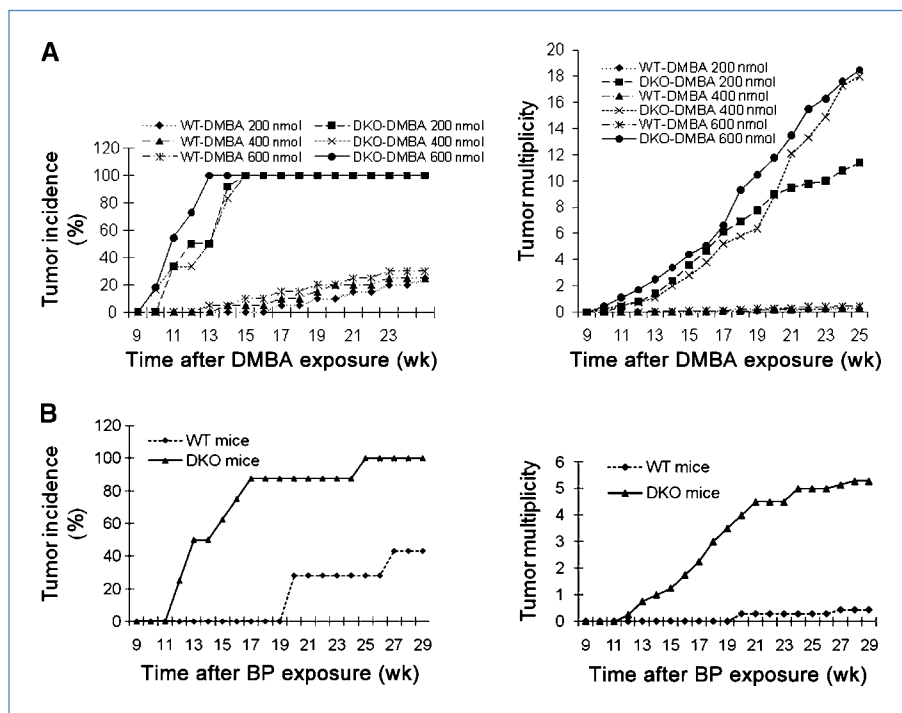


Figure 1. DMBA- and BP-induced skin tumor frequency and multiplicity. WT and DKO mice were exposed to indicated concentrations of DMBA or BP in a skin carcinogenesis model. The mice were analyzed for skin tumor frequency and multiplicity. A, DMBA-induced tumor incidence and tumor multiplicity per mouse. Table 1 shows mice with tumors per total mice in the group. B, BP-induced tumor incidence and tumor multiplicity per mouse.

one-way ANOVA, and mean values were compared using the Dunnett's test ($P < 0.05$).

Results

DMBA and BP induction of skin tumors in WT and DKO mice. We performed standard two-stage initiation-promotion experiments to study comparative susceptibility of WT and DKO mice to DMBA- and BP-induced skin tumors. Skin tumor incidence and tumor multiplicity were recorded (Fig. 1A and B; Table 1). The DKO mice showed significantly higher skin tumor incidences and multiplicity of tumors/mouse with all three (200, 400, and 600 nmol) doses of DMBA as compared with WT mice (Fig. 1A, left, top; Table 1). All the three doses led to development of skin tumors in 100% of DKO mice at week 14 after DMBA exposure (Fig. 1A, left, top). In contrast, <10% WT mice showed DMBA-induced skin tumors at week 14 after DMBA exposure. The highest tumor incidence in WT mice was 30%, with a maximum dose of 600 nmol DMBA.

The DKO mice exposed to DMBA showed early onset of skin tumors as compared with WT mice (Fig. 1A, left, top). The tumors in DKO mice started appearing at week 10 as compared with week 13 in case of WT mice. In the same experiment, WT and DKO mice exposed to vehicle or PMA alone failed to induce skin tumors. Interestingly, tumor multiplicity in DKO mice was significantly higher than WT mouse (Fig. 1A, right). DKO mice exposed to DMBA showed 10 to 18 tumors per mouse as compared with average of <0.2 tumor per WT mouse. DKO mice in two-stage carcinogenesis studies also showed significant increase in susceptibility to BP-induced skin carcinogenesis (Fig. 1B). DKO mice exposed to BP showed early onset of development of skin tumors as compared with WT mice (Fig. 1B, left). The tumor incidence in DKO mice reached 100% at week 25, but in WT mice, it only reached 43% at week 27. The tumor multiplicities at week 27 of DKO mice and WT mice were 5.28 and 0.43, respectively, showing significant difference between the two strains of mice ($P < 0.0001$; Fig. 1B, right).

Table 1. Mouse skin tumor incidence in response to DMBA

Treatment	Skin tumor incidence			
	Week 15		Week 25	
	WT	DKO	WT	DKO
DMBA (200 nmol)	0/20	24/24 ($P < 0.0001$)	5/20	24/24 ($P < 0.0001$)
DMBA (400 nmol)	1/20	24/24 ($P < 0.0001$)	5/20	24/24 ($P < 0.0001$)
DMBA (600 nmol)	2/20	22/22 ($P < 0.0001$)	6/20	22/22 ($P < 0.0001$)

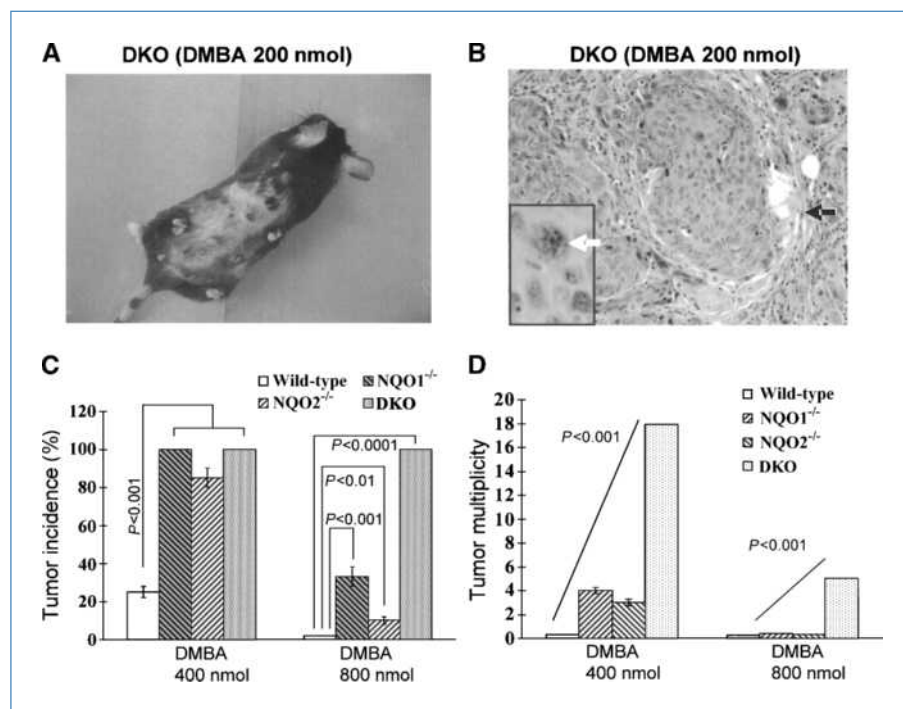
A representative tumor-bearing mouse exposed to 200 nmol DMBA is shown in Fig. 2A. The majority of the tumors that developed in the DKO mice were 4 mm in diameter, in contrast to the 1 mm or less size distribution observed in the WT population. Histologic evaluation of DMBA- and BP-induced skin tumors in WT and DKO mice showed that most tumors were typical exophytic, well-differentiated squamous cell papillomas. DKO mouse exposed to DMBA also showed a few squamous cell carcinomas as shown in Fig. 2B. The squamous cell carcinoma was not observed in WT mice treated with DMBA.

NQO1 and NQO2 single knockout mice exposed to DMBA and BP are known to develop low frequency of skin tumors as compared with WT mice (Fig. 2C; refs. 13–16). A comparison of DMBA- and BP-induced skin tumors and tumor multiplicities in DKO mice with WT, NQO1^{-/-}, and NQO2^{-/-} mice is plotted in Fig. 2C and D. DMBA exposure led to almost similar incidence of skin tumors in individual NQO1 and NQO2 knockout and DKO mice that were significantly higher than WT mice (Fig. 2C). However, BP treatment showed significantly higher incidence of tumors in DKO mice as compared with not only WT but also individual NQO1 and NQO2 knockout mice ($P < 0.0001$; Fig. 1C). Intriguingly, highly significant differences between DKO and individual NQO1 and NQO2 knockout mice exposed to DMBA and BP were observed in tumor multiplicity (Fig. 2D). DKO mice exposed to DMBA developed 10 to 18 tumors per mouse as compared with 3 to 4 tumors per NQO1^{-/-} and NQO2^{-/-} mouse. Similarly, the exposure to BP led to four or more tumors in DKO mouse as compared with a single tumor in NQO1^{-/-} and NQO2^{-/-} mice.

Immunohistologic analysis of growth, differentiation, and apoptosis factors. We used WT and DKO mice exposed

to acetone (vehicle control) and BP for 6, 12, and 24 hours to investigate the mechanism of increased susceptibility of DKO mice to develop skin tumors in response to BP (Figs. 3–5). The treated skin sections were analyzed for anti-p63, anti-p53, anti-ODC, anti-Bcl2, anti-Bax, and anti-caspase-3 antibodies by immunohistochemistry. Both p63 and p53 immunohistochemistry showed epithelial nuclear staining, whereas ODC, Bcl2, Bax, and caspase-3 showed cytoplasmic staining. The p63 and p53 cells with nuclear staining were counted and plotted (Figs. 3 and 4). Interestingly, BP treatment showed time-dependent increase in p63 in WT mice until 12 hours after exposure (Fig. 3). The p63 level dropped to basal level at 24 hours after BP exposure in WT mice. In contrast, DKO mice skin showed higher expression of p63 compared with WT mice and lack of induction of p63 at 6 and 12 hours after BP exposure (Fig. 3). The p63 showed increased expression in DKO mice but only at 24 hours after BP exposure (Fig. 3). WT mice skin showed low level of p53 staining that was absent in DKO mice (Fig. 4). WT mice treated with BP led to time-dependent increase in p53 at 12 and 24 hours after exposure. DKO mice in the same experiment showed induction of p53 only at 24 hours after BP exposure (Fig. 4). The induction of p53 was absent in DKO mice at 6 and 12 hours after BP exposure (Fig. 4). A comparison of WT and DKO mouse skin from various immunohistochemical analyses showed an intriguing observation of thinning of epithelium in DKO mice because of unknown reasons (Fig. 5). The immunohistochemical analysis also showed increased staining for proliferation marker ODC and anti-apoptotic protein Bcl2 as compared with WT mice at all three time points of BP exposure (Fig. 5A and B). However,

Figure 2. Phenotype and histotype of DKO tumor induced by 200 nmol DMBA and comparison of tumor frequency and multiplicity among DKO, NQO1^{-/-}, NQO2^{-/-}, and WT mice. A, gross appearance of skin tumors, which developed in DKO mouse. B, histotype of tumor: microscopic sections of skin showing well-differentiated squamous cell carcinoma from 200 nmol DMBA-treated group. Islands of squamous malignant cells (black arrow) are seen in which there is nuclear atypia and apoptosis (white arrow). A high mitotic ratio is also seen (H&E staining). Original magnification, $\times 20$. C, a comparison of DMBA- and BP-induced tumor incidence among WT, NQO1^{-/-}, NQO2^{-/-}, and DKO mice. D, a comparison of DMBA- and BP-induced tumor multiplicity among WT, NQO1^{-/-}, NQO2^{-/-}, and DKO mice.



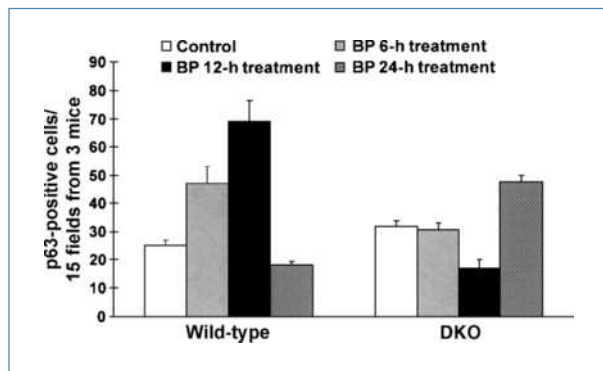


Figure 3. Immunohistochemical analysis of induction of p63 in BP-treated WT and DKO mice. Dorsal skin of WT and DKO mice was exposed to acetone or 800 nmol BP. Six, 12, and 24 h after BP treatment, the mice were euthanized and sections of treated skin were removed by surgery. Skin samples were fixed in formalin and embedded in paraffin, and sections were cut. Sections were analyzed by immunohistochemistry with anti-mouse p63 antibodies. The p63-positive cells were counted from 15 fields from three mice in each group. Columns, mean; bars, SD.

Bax and caspase-3 in the same experiment showed decreased staining in DKO mice skin compared with WT mice exposed to BP (Fig. 5C and D).

Western blot analysis. WT and DKO mice were exposed to acetone (vehicle control) and BP for 6, 12, 24, and 48 hours. The mice were euthanized, skin was collected by surgery and homogenized, and total cell lysate was analyzed by SDS-PAGE and immunoblotting for p53, p21, Bcl2, Bax, caspase-3, cleaved PARP, p19, c-Jun, ODC, PCNA, NQO1, NQO2, and actin (Fig. 6). NQO1 and NQO2 were present in WT mice but, as expected, were absent in DKO mice. The treatment with BP first increased and then decreased NQO1 and NQO2 in WT mice. DKO mice showed lower basal expression of tumor suppressor gene p53, growth arrest gene p21, and proapoptotic gene Bax but higher expression of antiapoptotic gene Bcl2 as compared with WT mice. The treatment with BP showed time-dependent increase in p53, p21, Bax, and caspase-3 in WT mice. However, the DKO mice exposed to BP showed delayed and smaller magnitude of increase in p53, p21, Bax, and caspase-3. In WT mice, the BP-induced skin samples showed higher PCNA levels as compared with DKO samples. The DKO mice also showed absence of cleaved PARP as observed in WT mice. WT mice showed significant increase in growth suppression gene p19 in response to BP. The increase in p19 was absent in DKO mice. The expression of proliferation-related genes c-Jun and ODC was undetected in WT mice. However, DKO mice in the same experiment showed time-dependent increase in c-Jun and higher expression of ODC.

Discussion

Previously, NQO1^{-/-} and NQO2^{-/-} mice exposed to DMBA and BP induced low frequency of skin tumors that was significantly higher than WT mice (13–16). This raised an interesting question about a combined role of NQO1 and NQO2 in preven-

tion of DMBA- and BP-induced skin carcinogenesis. We used DKO mice to investigate the combined role of NQO1 and NQO2 in prevention of skin carcinogenesis in response to carcinogens DMBA and BP. These studies were significant because DKO mice represented animal model for human individuals deficient in both NQO1 and NQO2 because of mutations in NQO1 gene and promoter polymorphism in NQO2 gene (18–20, 23, 24). DKO mice showed significantly higher sensitivity to develop skin tumors in response to DMBA and BP as compared with WT and individual knockout mice. The tumors developed early and were larger in size than individual knockout mice. One of the most intriguing observations was highly significant increase in tumor multiplicity. Most of the skin tumors in DKO and WT mice were papillomas. However, DKO mice showed a few carcinomas, which were absent in WT mice.

We also performed experiments to determine the mechanism of the role of NQO1/NQO2 in skin chemoprotection. We analyzed WT and DKO mice skin exposed to BP for factors that regulate growth/differentiation, proliferation, and apoptosis. These included p63, p53, p21, p19, Bcl2, Bax, caspase-3, c-Jun, and ODC. p63 family of factors is critical for epidermal morphogenesis and carcinogenesis (28–30). The p53 protein, called the guardian of the genome, represents a key regulator of the control of cell growth against internal and external stress through transcriptional-dependent and transcriptional-independent mechanisms (31–33). p53 is a tumor suppressor gene whose product can act as a suppressor of transformation (34) and is induced by DNA damage (35). In turn, p53 orchestrates a global transcriptional response that either counters cell proliferation or induces apoptosis (36). p21 is a critical regulator of the cell cycle, and cell fate in epidermis (37) was also induced after BP treatment. The accumulation of activated p53 protein induces a cell cycle arrest at the G₁ phase, which allows the

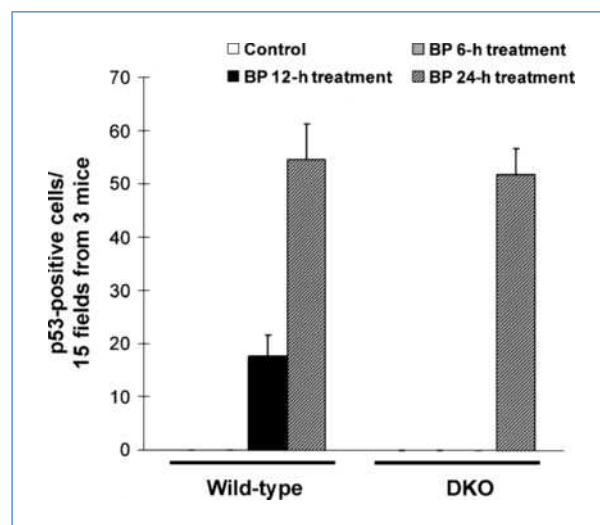


Figure 4. Immunohistochemical analysis of induction of p53 in BP-treated WT and DKO mice. Mice exposed to BP were analyzed by immunohistochemistry with anti-rabbit p53 antibody. The p53-positive cells were counted from 15 fields from three mice in each group. Columns, mean; bars, SD.

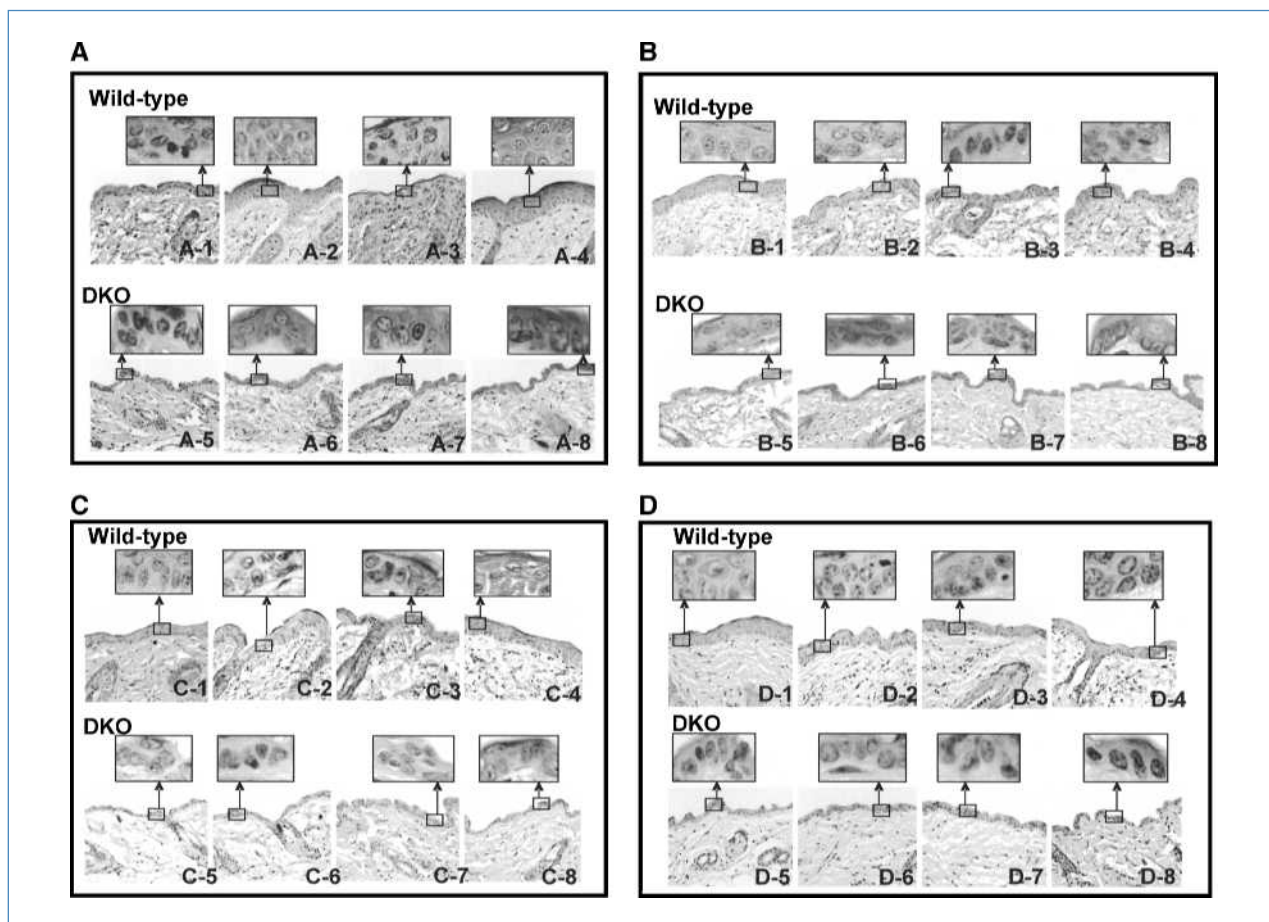


Figure 5. Immunohistochemical analysis of alterations in ODC, Bcl2, Bax, and caspase-3 in BP-treated WT and DKO mice. Mice exposed to BP were analyzed by immunohistochemistry with anti-mouse ODC (A), Bcl2 (B), Bax (C), and caspase-3 (D) antibodies. 1, WT vehicle exposed; 2 to 4, WT exposed with BP for 6 h (2), 12 h (3), and 24 h (4); 5, DKO mice vehicle treated; 6 to 8, BP-treated DKO mice for 6 h (6), 12 h (7), and 24 h (8).

repair of DNA damage before its replication in the S phase. In this pathway, p21 was discovered as an inhibitor of cyclin-dependent kinase (CDK), whose induction is associated with the expression of p53 (38). p21 mediates cell cycle arrest by binding to and inactivation of the cyclin D/CDK4, cyclin D/CDK6, and cyclin E/CDK2 complexes (38). Upregulation of p21 has also been documented in cells undergoing differentiation, senescence, and apoptosis, all processes that may negatively influence tumor formation or progression (39). A role for p21 as a downstream effector of p53-mediated tumor suppression is supported by its ability to block proliferation of p53-deficient tumor cells *in vitro* and *in vivo* (34). p19 suppresses growth, progression, and metastasis of tumor through p53-dependent and p53-independent pathways (40). Loss of p19 results in increased malignant conversion, more aggressive tumors, and frequent and rapid metastasis. However, one *in vivo* p19-null mouse model indicated additional p53-dependent tumor suppressor functions for p19 (40). The Bcl2 family of proteins consists of proapoptotic and antiapoptotic regulators of programmed cell death/apoptosis. The Bax gene is an apoptosis-promoting member of the Bcl2 gene family. The Bcl2 protein is known to form hetero-

dimers with the Bax protein *in vivo*, and the molar ratio of Bcl2 to Bax determines whether apoptosis is induced or inhibited in target tissues (41). The Bax protein is considered to be one of the primary targets of p53 and controls cell death through its participation in the disruption of mitochondria with the subsequent release of cytochrome c (41–43). Cytochrome c release, in turn, activates caspase-3, caspase-9, and PARP (42). Cleaved PARP is regarded as a proximate mediator of apoptosis. c-Jun is known to promote cellular proliferation (44). ODC is a key enzyme in cellular polyamine synthesis. Consequently, polyamine levels are elevated in the skin, which creates a cellular environment that greatly enhances tumor growth after minimal exposure to carcinogens (45). In DKO mice, the BP-induced samples showed lower PCNA levels as compared with WT samples. PCNA is associated with S phase of DNA replication (46). It is known that carcinogen administration induces resistance in cells, which can proliferate even under cytotoxic conditions as observed in BP-treated groups. The absence of normal cell proliferation activity seems to be responsible for the progression of papilloma to squamous cell carcinoma of the skin in DKO mice.

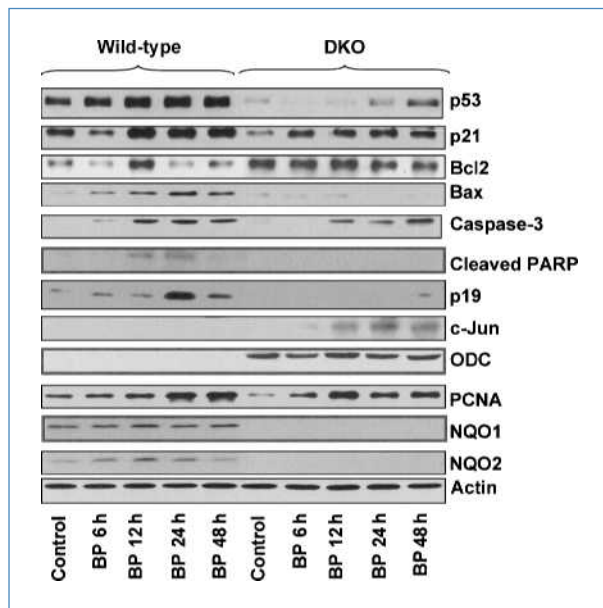


Figure 6. Western blot analysis. Dorsal skin of WT and DKO mice was shaved, and 2 d later, acetone or 800 nmol BP was applied on the shaved skin for indicated times. Skin samples from three mice in each group were combined. Samples from all groups were homogenized and analyzed by SDS-PAGE and Western blotting. Western blots were probed with p53, p21, Bcl2, Bax, caspase-3, cleaved PARP, p19, c-Jun, ODC, NQO1, NQO2, and actin antibodies.

Immunohistochemical analysis showed BP induction of p63 in WT mice that promoted differentiation of epidermal cells and protection against carcinogenesis. DKO mice showed delayed induction of p63 that might have interfered with normal process of differentiation and contributed to skin tumor development. The isoform of p63 that contributes to prevention of skin carcinogenesis in WT mice remains to be determined. The lower expression and delayed activation of tumor suppressor p53 and p19 also contributed to skin tumor development in DKO mice. This should also explain high occurrence of tumor multiplicity in DKO mice exposed to BP and DMBA. In addition, the increased expression of antiapoptotic protein Bcl2 and lack of optimal induction of tumor suppressor p53, proapoptotic protein Bax, and caspase-3 in DKO mice in response to BP suggested decreased apoptosis of damaged cells that also contributed to increased tumor incidence and multiplicity in DKO mice. This was also supported by the absence of cleaved PARP in DKO mice. Increase in c-Jun and ODC possibly promoted cellular proliferation, leading to tumor development in DKO mice.

PAHs undergo metabolic activation to exert their carcinogenic effects (1). BP is metabolized via cytochrome P450 system into reactive BP quinones and dihydrodiol epoxide derivatives (e.g., BP-7,8-dihydrodiol-9,10-epoxide). These metabolites bind covalently to DNA and form adducts, which may lead to mutations and consequently to uncontrolled cell growth and tumor formation in various tissues (1). DMBA is metabolized into its ultimate carcinogen, diol epoxide, by cytochrome P450 (2). P450 reactions generate reactive oxygen

species (ROS), leading to oxidative stress that is known to play a crucial role in the pathogenesis of cancer (47). Quinone oxidoreductases (NQO1 and NQO2) compete with cytochrome P450 and catalyze two-electron reduction of quinone metabolites of BP to hydroquinones, thus skipping one-electron reduction and semiquinone and ROS generation (48). Unlike BP, DMBA does not metabolically produce quinones, yet NQO1 and NQO2 protect mice against its carcinogenicity (14, 16). Therefore, the studies suggest that the role of NQO1 and NQO2 in protection against carcinogenicity is against all types of chemicals and not restricted to chemicals that are metabolized to quinones. The studies also suggest that mechanisms of NQO1 and NQO2 protection against chemical carcinogenesis involve not only detoxification of chemicals but also other mechanisms because they could protect against chemicals that are not substrates for NQO1 and NQO2.

One such mechanism of NQO1 and NQO2 protection is their role in stabilization of tumor suppressor p53 against 20S proteasomal degradation (49). This is due to direct physical interaction of NQO1 and NQO2 with p53 and reduction/abrogation of p53 interaction with 20S proteasomes. NQO1 and NQO2 are stress-inducible proteins and induced in response to chemical and radiation stress (49). This leads to NQO1- and NQO2-mediated stabilization of p53 and cellular protection. Therefore, it is possible that delayed/reduced activation of p53 in DKO mice in response to BP and DMBA treatment is due to loss of NQO1 and NQO2 stabilization of p53 against 20S degradation. NQO1 and NQO2 both were induced in response to BP, leading to stabilization/activation of p53 and protection against skin carcinogenesis. The role of NQO1 and NQO2 in control of stability of other factors, including p63 and p19, is expected but remains to be determined.

In summary, the results suggested that NQO1 and NQO2 combined provide protection against chemical-induced skin carcinogenicity. This protection is due to NQO1 and NQO2 control of factors that mediate cell growth and differentiation, proliferation, and apoptosis. This conclusion is significant for human individuals with combined deficiency of NQO1 and NQO2.

Disclosure of Potential Conflicts of Interest

No potential conflicts of interest were disclosed.

Acknowledgments

We thank Dr. Emmanuel Kalapurakal for help with immunohistochemical analysis.

Grant Support

National Institute of Environmental Health Sciences grant R01 ES07943. The costs of publication of this article were defrayed in part by the payment of page charges. This article must therefore be hereby marked *advertisement* in accordance with 18 U.S.C. Section 1734 solely to indicate this fact.

Received 8/8/09; revised 10/15/09; accepted 11/13/09; published OnlineFirst 1/26/10.

References

- International Agency for Research on Cancer (IARC). IARC monographs on the evaluation of carcinogenic risks of chemicals to humans—polynuclear aromatic compounds, vol. 32 (33-91). pp. 211–24. Lyon: International Agency for Research on Cancer Scientific Publications; 1983.
- Pugalendhi P, Manoharan S, Panjamurthy K, Balakrishnan S, Nirmal MR. Antigenotoxic effect of genistein against 7,12-dimethylbenz[a]anthracene induced genotoxicity in bone marrow cells of female Wistar rats. *Pharmacol Rep* 2009;61:296–303.
- Prince M, Campbell CT, Robertson TA, Wells AJ, Kleiner HE. Naturally occurring coumarins inhibit 7,12-dimethylbenz[a]anthracene DNA adduct formation in mouse mammary gland. *Carcinogenesis* 2006;27:1204–13.
- Housman TS, Feldman SR, Williford PM, et al. Skin cancer is among the most costly of all cancers to treat for the medicare population. *J Am Acad Dermatol* 2003;48:425–9.
- Ross D. Quinone reductases multitasking in the metabolic world. *Drug Metab Rev* 2004;36:639–54.
- Wu K, Knox R, Sun XZ, et al. Catalytic properties of NAD(P)H:quinone oxidoreductase-2(NQO2), a dihydronicotinamide riboside dependent oxidoreductase. *Arch Biochem Biophys* 1997;345:221–8.
- Zhao Q, Yang XL, Holtzclaw WD, Talalay P. Unexpected genetic and structural relationship of a long-forgotten flavoenzyme to NAD(P)H:quinone reductase (DT-diaphorase). *Proc Natl Acad Sci U S A* 1997;94:1669–74.
- Knox RJ, Jenkins TC, Hobbs SM, Chen S, Melton RG, Burke PJ. Bioactivation of 5-(aziridin-1-yl)-2,4-dinitrobenzamide (CB1954) by human NAD(P)H quinone oxidoreductase 2: a novel co-substrate-mediated antitumor prodrug therapy. *Cancer Res* 2000;60:4179–86.
- Radjendirane V, Joseph P, Lee H, et al. Disruption of the DT diaphorase (NQO1) gene in mice leads to increased menadione toxicity. *J Biol Chem* 1998;273:7382–9.
- Long DJ, Iskander K, Gaikwad A, et al. Disruption of dihydronicotinamide riboside:quinone oxidoreductase 2 (NQO2) leads to myeloid hyperplasia of bone marrow and decreased sensitivity to menadione toxicity. *J Biol Chem* 2002;277:46131–9.
- Gaikwad A, Long DJ, Stringer JL, Jaiswal AK. *In vivo* role of NAD(P)H:quinone oxidoreductase 1 (NQO1) in the regulation of intracellular redox state and accumulation of abdominal adipose tissue. *J Biol Chem* 2001;276:22559–64.
- Long DJ II, Gaikwad A, Multani A, et al. Disruption of the NAD(P)H:quinone oxidoreductase 1 (NQO1) gene in mice causes myelogenous hyperplasia. *Cancer Res* 2002;62:3030–6.
- Long DJ II, Waikel RL, Wang X, Perlaky L, Roop DR, Jaiswal AK. NAD(P)H:quinone oxidoreductase 1 deficiency increases susceptibility to benzo(a)pyrene-induced mouse skin carcinogenesis. *Cancer Res* 2000;60:5913–5.
- Long DJ, Walkel RL, Wang X, Roop DR, Jaiswal AK. NAD(P)H:quinone oxidoreductase 1 deficiency and increased susceptibility to 7,12-dimethylbenz(a)anthracene-induced carcinogenesis in mouse skin. *J Natl Cancer Inst* 2001;93:1166–70.
- Iskander K, Paquet M, Brayton C, Jaiswal AK. Deficiency of NRH:quinone oxidoreductase 2 increases susceptibility to 7,12-dimethylbenz(a)anthracene and benzo(a)pyrene-induced skin carcinogenesis. *Cancer Res* 2004;64:5925–8.
- Iskander K, Gaikwad A, Paquet M, et al. Lower induction of p53 and decreased apoptosis in NQO1-null mice lead to increased sensitivity to chemical-induced skin carcinogenesis. *Cancer Res* 2005;65:2054–8.
- Jaiswal AK, Bell DW, Radjendirane V, Testa JR. Localization of human NQO1 gene to chromosome 16q22 and NQO2-6p25 and associated polymorphisms. *Pharmacogenetics* 1999;9:413–8.
- Anwar A, Dehn D, Siegel D, et al. Interaction of human NAD(P)H:quinone oxidoreductase 1 (NQO1) with the tumor suppressor protein p53 in cells and cell-free systems. *J Biol Chem* 2003;278:10368–73.
- Rothman N, Smith MT, Hayes RB, et al. Benzene poisoning, a risk factor for hematological malignancy, is associated with the NQO1 609C→T mutation and rapid fractional excretion of chlorzoxazone. *Cancer Res* 1997;57:2839–42.
- Larson RA, Wang Y, Banerjee M, et al. Prevalence of the inactivating 609C→T polymorphism in the NAD(P)H:quinone oxidoreductase (NQO1) gene in patients with primary and therapy-related myeloid leukemia. *Blood* 1999;94:803–7.
- Jaiswal AK. Human NAD(P)H:quinone oxidoreductase (NQO1) gene structure and induction by dioxin. *Biochemistry* 1991;30:10647–53.
- Iida A, Sekine A, Saito S, et al. Catalog of 320 single nucleotide polymorphisms(SNPs) in 20 quinone oxidoreductase and sulfotransferase genes. *J Hum Genet* 2001;46:225–40.
- Wang W, Jaiswal AK. Sp3 repression of polymorphic human NRH:quinone oxidoreductase 2 gene promoter. *Free Radic Biol Med* 2004;37:1231–43.
- Harada S, Fujii C, Hayashi A, Ohkoshi N. An association between idiopathic Parkinsons disease and polymorphisms of phase II detoxification enzymes: glutathione S-transferase M1 and quinone oxidoreductase 1 and 2. *Biochem Biophys Res Commun* 2001;288:887–92.
- Das A, Kole L, Wang L, Barrios R, Moorthy B, Jaiswal AK. BALT development and augmentation of hyperoxic lung injury in mice deficient in NQO1 and NQO2. *Free Radic Biol Med* 2006;40:1843–56.
- DiGiovanni J. Multistage carcinogenesis in mouse skin. *Pharmacol Ther* 1992;54:63–128.
- Bogovaski P. Tumours of the skin. In: Tutusov VS, Dells Porta G, editors. Pathology of tumours in laboratory animals, volume 2—tumors of the mouse. Lyon: International Agency for Research on Cancer Scientific Publications; 1979, p. 1–45.
- Koster MI, Dai D, Roop DR. Conflicting roles for p63 in skin development and carcinogenesis. *Cell Cycle* 2007;6:269–73.
- Guo X, Mills AA. p63, cellular senescence and tumor development. *Cell Cycle* 2007;6:305–11.
- Koster MI, Lu SL, White LD, Wang XJ, Roop DR. Reactivation of developmentally expressed p63 isoforms predisposes to tumor development and progression. *Cancer Res* 2006;66:3981–6.
- Pietsch EC, Humberly O, Murphy ME. Polymorphisms in the p53 pathway. *Oncogene* 2006;25:1602–11.
- Oren M, Bartek J. The sun side of p53. *Cell* 2007;128:826–8.
- Sun Y. p53 and its downstream proteins as molecular targets of cancer. *Mol Carcinog* 2006;45:409–15.
- Finlay CA, Hinds PW, Levine AJ. The p53 proto-oncogene can act as a suppressor of transformation. *Cell* 1989;57:1083–93.
- Kastan MB, Onyekwere O, Sidransky D, Vogelstein B, Craig RW. Participation of p53 protein in the cellular response to DNA damage. *Cancer Res* 1991;51:6304–11.
- Sheer CJ. Principles of tumor suppression. *Cell* 2004;116:235–46.
- Patel R, Krishnan R, Ramchandani A, Maru G. Polymeric black tea polyphenols inhibit mouse skin chemical carcinogenesis by decreasing cell proliferation. *Cell Prolif* 2008;41:532–53.
- Melnikova VO, Ananthaswamy HN. Cellular and molecular events leading to the development of skin cancer. *Mutat Res* 2005;571:91–106.
- Weinberg WC, Fernandez-Salas E, Morgan DL, et al. Genetic deletion of p21WAF1 enhances papilloma formation but not malignant conversion in experimental mouse skin carcinogenesis. *Cancer Res* 1999;59:2050–4.
- Kelly-Spratt KS, Gurley KE, Yasui Y, Kemp CJ. p19Arf suppresses growth, progression, and metastasis of Hras-driven carcinomas through p53-dependent and independent pathways. *PLoS Biol* 2004;2:1138–49.
- Oltvai ZN, Milliman CL, Korsmeyer SJ. Bcl-2 heterodimerizes *in vivo* with a conserved homolog, Bax, that accelerates programmed cell death. *Cell* 1993;74:609–19.
- Marzo I, Brenner C, Zamzami N, et al. Bax and adenine nucleotide translocator cooperate in the mitochondrial control of apoptosis. *Science* 1998;281:2027–31.

43. Wang X. The expanding role of mitochondria in apoptosis. *Genes Dev* 2001;15:2922–33.
44. Jochum W, Passequé E, Wagner EF. AP-1 in mouse development and tumorigenesis. *Oncogene* 2001;20:2401–12.
45. O'Brien TG, Megosh LC, Gilliard G, Soler AP. Ornithine decarboxylase overexpression is a sufficient condition for tumor promotion in mouse skin. *Cancer Res* 1997;57:2630–7.
46. Motiwale L, Ingle AD, Rao KV. Mouse skin tumor promotion by sodium arsenate is associated with enhanced PCNA expression. *Cancer Lett* 2005;223:27–35.
47. Simic MG. DNA markers of oxidative processes *in vivo*: relevance to carcinogenesis and anticarcinogenesis. *Cancer Res* 1994;54:1918–23S.
48. Radjendirane V, Joseph P, Jaiswal AK. Gene expression of DT-diaphorase (NQO1) in cancer cells. In: Forman HJ, Cadenas E, editors. *Oxidative stress and signal transduction*. New York: Chapman and Hall; 1997, p. 441–75.
49. Gong X, Kole L, Iskander K, Jaiswal AK. NRH:quinone oxidoreductase 2 and NAD(P)H:quinone oxidoreductase 1 protect tumor suppressor p53 against 20S proteasomal degradation leading to stabilization and activation of p53. *Cancer Res* 2007;67:5380–8.

Cancer Research

The Journal of Cancer Research (1916–1930) | The American Journal of Cancer (1931–1940)

Inactivation of the Quinone Oxidoreductases NQO1 and NQO2 Strongly Elevates the Incidence and Multiplicity of Chemically Induced Skin Tumors

Jun Shen, Roberto J. Barrios and Anil K. Jaiswal

Cancer Res 2010;70:1006-1014. Published OnlineFirst January 26, 2010.

Updated version Access the most recent version of this article at:
doi:[10.1158/0008-5472.CAN-09-2938](https://doi.org/10.1158/0008-5472.CAN-09-2938)

Cited articles This article cites 46 articles, 20 of which you can access for free at:
<http://cancerres.aacrjournals.org/content/70/3/1006.full.html#ref-list-1>

Citing articles This article has been cited by 8 HighWire-hosted articles. Access the articles at:
</content/70/3/1006.full.html#related-urls>

E-mail alerts [Sign up to receive free email-alerts](#) related to this article or journal.

Reprints and Subscriptions To order reprints of this article or to subscribe to the journal, contact the AACR Publications Department at pubs@aacr.org.

Permissions To request permission to re-use all or part of this article, contact the AACR Publications Department at permissions@aacr.org.